Microscopic mechanisms of the growth of metastable silver icosahedra

F. Baletto,[1] C. Mottet,[2] and R. Ferrando[1,*]
[1]*INFM and CFSBT/CNR, Dipartimento di Fisica dell'Università di Genova, via Dodecaneso 33, 16146 Genova, Italy*
[2]*CRMC2/CNRS, Campus de Luminy, Case 913, 13288 Marseille Cedex 9, France*
(Received 17 November 2000; published 26 March 2001)

The growth of free silver nanoclusters is investigated by molecular-dynamics simulations up to sizes close to $N=600$ atoms on realistic time scales, and in a temperature range from 400 to 650 K. At low and intermediate temperatures, we grow mainly noncrystalline structures, as icosahedra and decahedra. In particular, at $N>200$, we obtain that perfectly ordered metastable icosahedra are very likely grown: either by a shell-by-shell mode on a small-size stable icosahedron, or by a complete structural transformation from a decahedron to a metastable icosahedron. The latter mechanism can explain why large silver icosahedra are more abundant than large decahedra in experiments. At high temperatures, crystalline fcc clusters are very frequently grown.

DOI: 10.1103/PhysRevB.63.155408 PACS number(s): 61.46.+w

I. INTRODUCTION

The study of the properties of small metal particles is of fundamental importance due to their applications in catalysis and surface nanostructuring.[1–3] In this field, the study of how the structure of free clusters develops as a function of their size is a key step to understanding their physical and chemical properties.[4,5] Clusters can be grown by different experimental methods,[6] and their final arrangement is the result of a competition between thermodynamic and kinetic factors.[7] In the case of metal nanoclusters, both crystalline (fcc for silver) and noncrystalline structures, like icosahedra and decahedra (see Fig. 1),[4,5] have been observed. One of most puzzling results in the field of free clusters growth is the finding of large silver icosahedra (Ih) in inert gas aggregation (IGA) sources experiments.[8] There, an abundance of icosahedra has been found, at such large sizes at which these structures are thought not to be the most favorable ones from the energetic point of view. Icosahedra (see Fig. 1) are quasispherical, noncrystalline structures, where atoms are arranged in concentric shells.[5] Icosahedra present six fivefold symmetry axes and are limited by close-packed distorted (111)-like facets. Icosahedra are thus able to minimize efficiently the cluster surface energy, but at the expense of the internal strain,[4,9,10] so that they become energetically unfavorable when the bulk contribution to the excess energy overcomes the surface contribution. On the other hand, the decahedra (Dh),[4,5] which have a single fivefold axis, are less spherical than the icosahedra, but have less internal strain,[9] and in the Marks-truncated form (m-Dh, see Refs. 4,7,11 and Fig. 1) they can optimize quite well the surface energy. Finally, crystalline clusters [fcc truncated octahedra (TO) for silver, copper, nickel, etc., see Fig. 1] have no internal strain but rather large surface energy, because of the wide (100) facets that are necessary to build up a quasispherical structure. Therefore, it often happens that icosahedral structures are the most stable at small sizes, decahedra are favorable at intermediate sizes, and crystalline structures are recovered in the limit of large objects. As an example, total-energy calculations on nickel have shown that the best structures are icosahedra at sizes $N<2300$, decahedra at $2300<N<17\,000$, and fcc polyhedra at larger N.[9] For a more detailed discussion of small sizes ($N\leqslant 75$) see Refs. 12,13. Magic numbers for Dh, Ih, and fcc structures are listed in Table I. Due to the above facts, the experimental detection[8] of large (several thousands of atoms) silver icosahedra suggests that they are growth, and not equilibrium, structures. However, in the same experiment, small clusters (~ 2 nm of diameter, corresponding to N in the range 100–200 atoms) are mainly decahedra, while large icosahedra are more abundant than large decahedra. The explanation of this finding is not yet clear.

In Ref. 7, we have studied by molecular-dynamics (MD) simulations, the growth of silver clusters at small sizes ($N<150$ atoms). There, we have shown that, at $N\simeq 150$, icosahedral structures are indeed energetically favorable, and that it is possible to grow metastable decahedra in a wide range of growth conditions (temperature T and deposition flux ϕ), in competition with the stable icosahedra. In this paper, we simulate the growth at larger sizes, where icosahedra become unfavorable, and show how it is possible to grow metastable icosahedra. In fact, we shall show by energy optimization that icosahedral structures begin to have larger energies than decahedral clusters already at sizes below 200 atoms. In spite of that, our MD simulations shall demonstrate that, at a given ϕ, there is a T range in which it is likely that metastable (and almost perfectly ordered) icosahedral structures grow. We show that these metastable icosahedra can be grown by different microscopic mechanisms, either involving an almost shell-by-shell growth (already guessed in Ref. 14) on a preexisting stable icosahedron of smaller size, or, more surprisingly, and of more importance, involving a complete restructuring from decahedron to icosahedron. This kinetic Dh $\rightarrow$ Ih transformation, which goes in the opposite direction with respect to what is suggested by energetic considerations, is crucial to explain why large icosahedra are more abundant than large decahedra in experiments. Moreover, we shall investigate the possibility of growing fcc structures, showing that the latter are more frequently found at high temperatures, in agreement with the IGA experiments.[8]

Apart from being suited for studying kinetic effects,

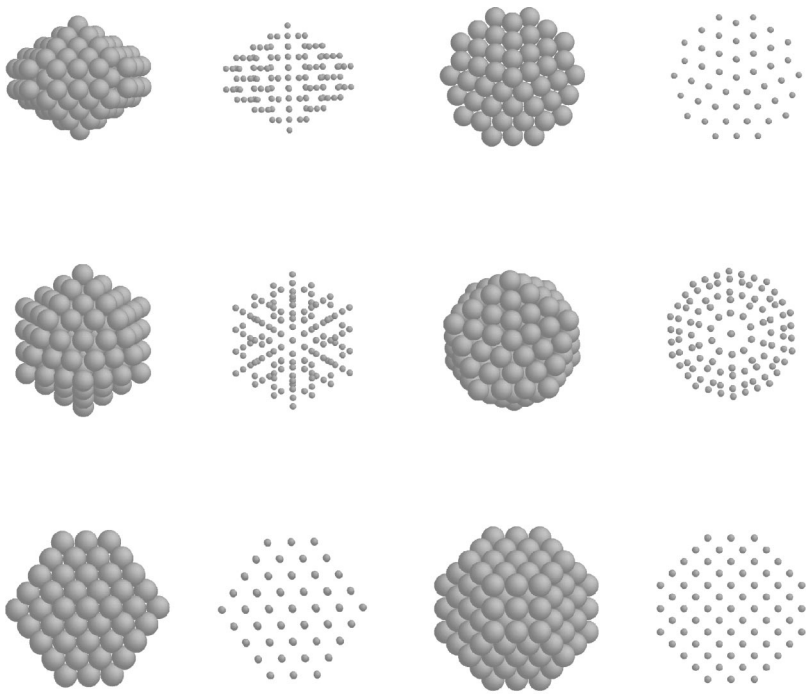

FIG. 1. Decahedral (top row), icosahedral (middle row), and fcc truncated octahedral structures (bottom row). Each structure is shown in side (first two columns of the figure) and top views (third and fourth columns), and each view is given in two representations. In the first row, the 146 Marks truncated decahedron is shown. For this decahedron $(m,n,p)=(3,2,2)$. Remember that *m* and *n* are the width and the height of the rectangular (100)-like facets (see the side view in the first figure of the first row) respectively, while *p* is the depth of the Marks reentrance. The top and the bottom of the decahedron are both formed by five close-packed (111) facets, arranged around the fivefold symmetry axis (see the third figure of the first row). Notice that from the top view, the atoms of the decahedron appear to be perfectly arranged in columns, as can be clearly seen in the fourth figure in the first row. This is what we call *decahedral stacking*. This stacking is the fcc-like stacking on the distorted (111) facets. In the second row, the 147 icosahedron is shown. The top view (which is taken starting from one of the 12 fivefold vertices) shows well that the inner arrangement of atoms is quite different from the decahedral case. The third row shows the 201 truncated octahedron. No fivefold symmetries are present.

growth simulations are also a powerful tool for helping the search for the most stable structures as a function of the size, and in particular, at the difficult sizes (i.e., at the ones that are far from magic numbers). Moreover, the growth simulations give information on the effects of temperature on these structures.

The paper is structured as follows. Section II contains a short description of the simulation procedure and of the method for analyzing the structures. Section III contains a brief summary of the results at small sizes (which were treated in more detail in Ref. 7). Sections IV and V contain the results, which have been obtained at larger sizes; Sec. IV is focused on the growth modes of metastable icosahedra, and Sec. V is devoted to the growth of fcc clusters. Finally, Sec. VI contains the discussion and conclusions.

II. MODEL AND METHODS

In our simulations, silver is modeled by many-body potentials as developed in the framework of the second-moment approximation to the tight-binding model.[15] The form and the parameters of the potentials are given in Ref. 16. These potentials have been successfully used in the modeling of structural and dynamical properties of transition and noble-metal surfaces.[17–23] In our growth simulations, we deposit atoms one by one with a time interval $\tau=\phi^{-1}$; in between two subsequent depositions, all cluster atoms are free to move. Each is deposited by putting it randomly on a large sphere centered around the cluster, and by giving it a velocity directed towards the cluster. That velocity is chosen to correspond to the typical average kinetic energy of the vapor atoms in IGA sources. In the following, we fix $\tau=7$ ns, if not otherwise specified. This deposition time is quite close to those in IGA sources, being, however, somewhat faster (for a discussion of this point, see Ref. 7). During the growth simulation, the cluster is kept at a constant temperature by an Andersen thermostat, whose collision frequency is chosen in order to insure efficient thermalization without altering the diffusive properties of the atoms in the cluster.[16] We choose to simulate temperature interval $350<T<650$ K, in agreement with the few available estimates of cluster temperatures in IGA sources.[24] The energetics of perfect structures is studied by quenched molecular-dynamics simulations. The diffusion barriers for adatoms on cluster surfaces are calculated by the nudged elastic band (NEB) method.[25] The NEB method is necessary in particular when dealing with multiple-exchange processes, such as the chain process,[14,16] which is important on Marks decahedra (see the following).

The cluster structure during growth is monitored by the

TABLE I. Size N, type of structure, length of the fivefold symmetry axes N_5 (in atoms), and percentages P of the occurrences of the CNA signatures (5,5,5), (4,2,1), and (4,2,2).

N	Structure	N_5	$P(5,5,5)$	$P(4,2,1)$	$P(4,2,2)$
75	(2,2,2) m-Dh	5	1.25	28.2	20.4
100	(3,1,2) m-Dh	5	0.92	27.6	19.6
101	(2,3,2) m-Dh	6	1.12	33.7	20.2
146	(3,2,2) m-Dh	6	0.75	39.6	18.7
192	(3,3,2) m-Dh	7	0.66	45.3	18.2
212	(2,2,3) m-Dh	7	0.60	44.7	16.4
238	(3,4,2) m-Dh	8	0.61	48.6	18.0
247	(4,2,2) m-Dh	7	0.51	47.2	16.9
268	(2,3,3) m-Dh	8	0.54	48.6	15.8
318	(4,3,2) m-Dh	8	0.45	52.5	16.3
55	Ih	5	10.3	0.00	38.5
147	Ih	7	5.17	17.2	38.8
309	Ih	9	3.10	31.0	34.9
561	Ih	11	2.06	41.2	30.9
116	TO		0.00	60.5	0.00
201	TO		0.00	64.6	0.00
225	TO		0.00	61.8	0.00
314	TO		0.00	68.0	0.00

common neighbor analysis (CNA).[26] We assign to each pair of nearest-neighbor atoms a CNA signature, i.e., a triplet of integers (r,s,t) (do not confuse them with the triplet of integers describing the truncation in the m-Dh structures[11]). r is the number of common nearest neighbors of two atoms of the pair, s is the number of nearest-neighbor bonds among the r common nearest neighbors, and t is the length of the longest chain that can be formed with the s bonds.[26,27] We have found that the monitoring of the signatures $(r,s,t)=(5,5,5),(4,2,1),(4,2,2)$ is sufficient to distinguish icosahedral, decahedral, and fcc structures in the size range of our simulations. In Table I we report the percentages $P(5,5,5)$, $P(4,2,1)$, and $P(4,2,2)$ of the above signatures over the total number of signatures in the cluster (i.e., over the total number of nearest-neighbor pairs in the cluster), for several perfect structures at magic numbers. In particular, $P(5,5,5)$ is important to identify local fivefold symmetries. In fact, the pairs of nearest-neighbor atoms that are located along a (locally) fivefold axis, are characterized by the (5,5,5) signature. Because of that, $P(5,5,5)$ is much larger in icosahedra than in decahedra of comparable size (the ratio between the numbers of fivefold axes in Ih and Dh structures is 6 to 1), and it is zero in fcc clusters. In our growth simulations we have monitored the above CNA signatures by analyzing at least 100 snapshots at each size N and then averaging over these snapshots.

III. RESULTS AT SMALL SIZES ($N<150$)

The growth of silver cluster at sizes $N<150$ (Ref. 7) can be summarized as follows. At low temperatures (350–400 K), after passing through well-ordered icosahedral and decahedral structures at the magic numbers of 55 and 75 atoms,

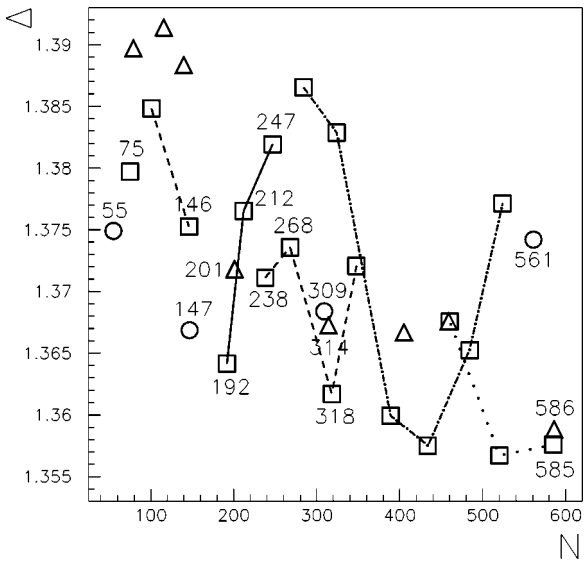

FIG. 2. Energetics of clusters for $N<600$. Parameter $\Delta=[E(N)-N\epsilon_B]/N^{2/3}$, where $E(N)$ is the optimized energy of a cluster of size N and ϵ_B is the cohesive bulk energy per atom, as a function of N. The circles, squares, and triangles refer to icosahedral, decahedral, and fcc (truncated octahedral) structures. The lines join decahedral structures with the same number N_5 of atoms along the symmetry axis: 7 (full line), 8 (dashed line), 9 (dash-dotted line), and 10 (dotted line) atoms.

respectively, the growth ends up preferentially with icosahedra at $N\simeq150$, even if sometimes either decahedra or hybrid structures are found. At these low temperatures, the transformation from the 75 decahedron to the 147 icosahedron takes place via the formation of an external icosahedral shell. We remark here that most of the low-temperature ''hybrid structures'' in Table I of Ref. 7 are indeed decahedra with external icosahedral shells, which are undergoing a transformation directly to the 309 Ih without forming the 147 Ih (see the next section for a discussion of these kinds of transformations). At intermediate temperatures ($450<T<550$ K), the results are practically the same as at lower temperatures in the range $N<100$, while at $N\simeq150$, metastable decahedra are by far the most likely outcome of the growth process. At higher temperatures ($T>550$ K), we encountered melted structures up to $N\simeq130$, and the final outcome at $N\simeq150$ are icosahedra (the best structures in this size range from the energetic point of view). By varying the deposition flux, the transition temperatures at $N\simeq150$ are somewhat displaced. This reentrant morphology transition[7] is due to the competition between two magic structures, a Marks truncated decahedron at 146 atoms and an icosahedron at 147 atoms.

IV. RESULTS AT $N>150$: GROWTH MODES OF METASTABLE ICOSAHEDRA

Before dealing with the growth simulations results at larger sizes, we discuss the energetics of perfect structures up to $N\simeq600$, as obtained after relaxation by quenched MD. In Fig. 2, we report the quantity Δ, defined as

$$\Delta = \frac{E_N - \varepsilon_B N}{N^{2/3}} \quad (1)$$

(where E_N is the optimized energy of a cluster of size N and ε_B is the cohesive energy per atom in bulk Ag), for several magic structures of different symmetries (the squares, circles, and triangles refer to Dh, Ih, and fcc structures, respectively). Decahedral structures with the axis of the same length N_5 are connected by lines. The quantity Δ can be roughly interpreted as the ratio between the excess energy (due to surface contributions and to internal contributions, the latter due to strain) and the number of surface atoms (which is approximately $N^{2/3}$).[9] For decahedral and icosahedral structures, Δ first decreases with N, then reaches a minimum, and asymptotically increases, because the strain contribution is proportional to N.[9] For fcc structures, there is only the surface contribution, and Δ keeps on decreasing to approach a constant limit. In Fig. 2, it can be seen that Δ begins to increase for icosahedral structures already after the 147 Ih, while it is possible to single out a sequence of low-energy decahedral perfect structures whose Δ decreases up to $N \sim 10\,000$.[28] In particular, in the range $180 < N < 600$, perfect decahedra display the most favorable Δ values compared to other structures, sometimes in rather close competition with fcc structures. This suggests that, at different sizes from magic numbers (see Table I for the list of magic numbers), imperfect decahedra (or, in narrower size ranges, imperfect fcc structures) should be the energetically favorable structures. On the other hand, icosahedra are not favorable. Only at $N = 309$ (a magic number for icosahedra) were we not able to find any imperfect decahedron or fcc cluster better than the perfect icosahedron. But as we move away from 309, at $N = 308$ and 310, there are imperfect decahedra that are more favorable than the best icosahedron. On the other hand, at $N = 561$, which is the subsequent magic number for icosahedra, we have found several imperfect decahedra and fcc clusters of lower energy than the perfect icosahedron [the decahedra are obtained by eliminating 24 atoms from the 585 (5,4,2) m-Dh, the fcc clusters are obtained eliminating 25 atoms from a 586 symmetric truncated octahedron].

The above picture is confirmed by the results of high-T growth simulations, where the growth sequence is expected to be rather close to the stable-structure sequence, since the cluster has more chances to optimize its free energy. At high T (we tried 600 and 650 K), we have made several simulations up to $N = 325$, and sometimes to larger sizes, never obtaining icosahedral structures for $N > 180$. We have obtained, always, decahedral structures at 600 K, while fcc clusters have been frequently grown at 650 K. At the latter temperature, entropy effects are thus becoming very important (see the next section for a discussion).

Let us consider, for example, a typical simulation at $T = 600$ K (see Figs. 3 and 4). We recall that at 600 K, silver clusters grow as icosahedra at $N \simeq 150$.[7] The deposition of some tens of atoms on the 147 icosahedron causes a quite sharp transition to decahedral structures around $N \simeq 170$. In fact, at $N = 192$ (third snapshot in Fig. 3), the (3,3,2) m-Dh is a very stable structure (see Fig. 2). The CNA analysis of Fig.

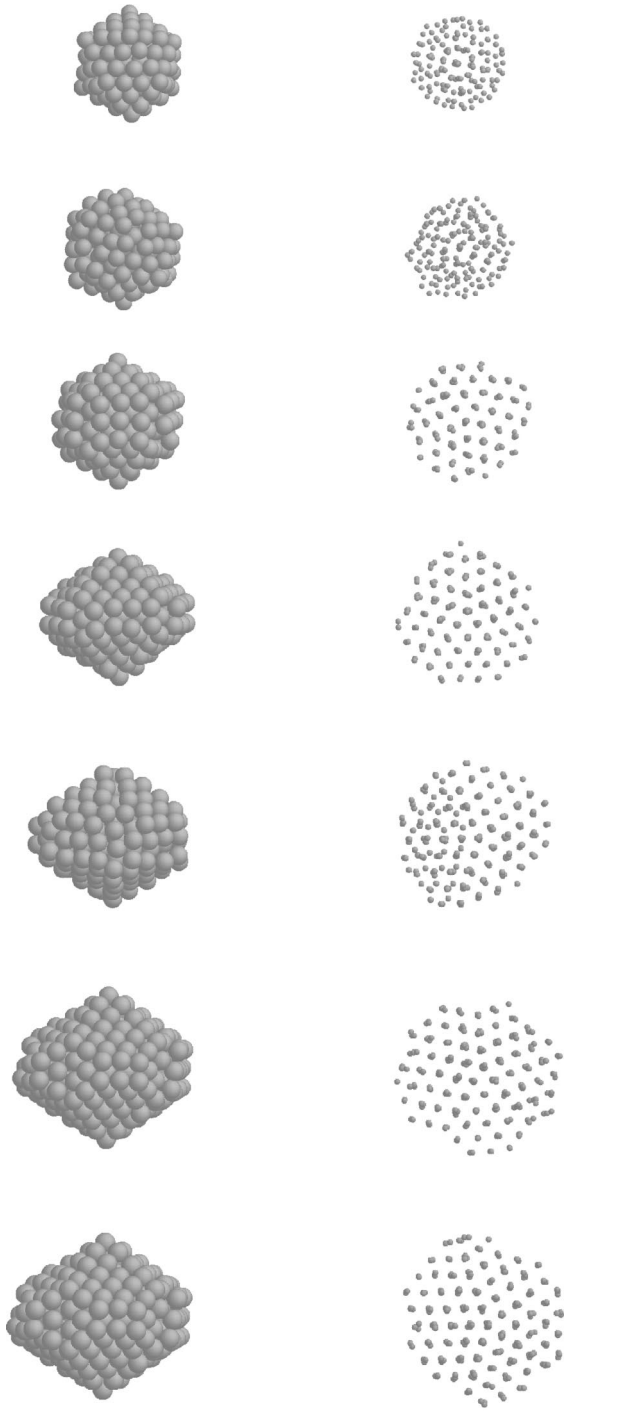

FIG. 3. Growth at 600 K. From the top to the bottom row, seven snapshots are taken at $N = 147$, 166, 192, 220, 257, 310, 324 atoms, and each snapshot is shown both in side and top view. In the first snapshot (first row), the structure is icosahedral. In between the second ($N = 166$) and the third snapshot ($N = 192$), there is a transition to a decahedral structure, and then the structure keeps growing as a decahedron. Notice that in the fifth snapshot ($N = 257$) an island has grown on the top of the decahedron. This island is not in decahedral stacking (since it breaks the arrangement in columns of the structure) but in icosahedral stacking. Decahedral and icosahedral stackings correspond to fcc and hcp stackings on the (111) facets, respectively.

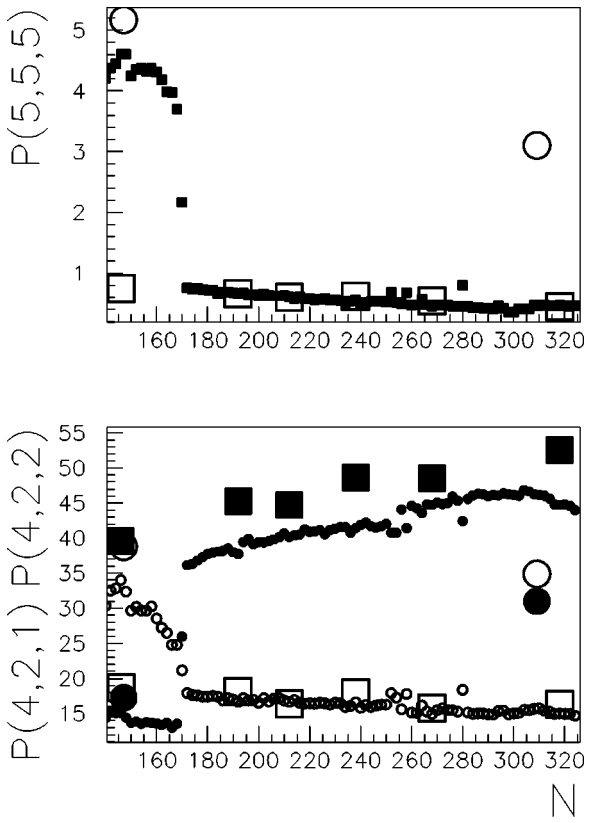

FIG. 4. Common-neighbor analysis of the simulation in Fig. 3. The small dots represent the simulation results, while the big symbols (squares, circles, and triangles) are the values corresponding to the perfect structures at magic numbers (see Table I). In particular, squares refer always to decahedral structures, circles to icosahedral structures, and triangles (not shown in this figure) to fcc structures. In the lower panel, $P(4,2,1)$ is represented by the small black dots for what concerns the simulation results, and by the filled symbols for what concerns the magic structures. $P(4,2,2)$ is represented by the small open dots for what concerns the simulation results, and by the open symbols for what concerns the magic structures. The transition from icosahedral to decahedral structures around $N=170$ causes a drop of $P(5,5,5)$ and of $P(4,2,2)$, with the simultaneous rise of $P(4,2,1)$.

4 indicates clearly the transition from the icosahedral to the decahedral symmetry by a drop in $P(5,5,5)$ and in $P(4,2,2)$, with a simultaneous increase of $P(4,2,1)$. This Ih $\rightarrow$ Dh transition involves the formation of a quasimelted intermediate structure, which suddenly transforms into a decahedron. Going on with the growth, the cluster passes through different decahedral structures. First, the truncations are somewhat filled (see the fourth snapshot of Fig. 3, which is taken at $N=220$), and the cluster develops along the line connecting to the 212 (2,2,3) and (almost) the 247 (4,2,2) m-Dh (thus preserving $N_5=7$); then a new layer nucleates (see below) so that the cluster grows to the 318 (4,3,2) m-Dh ($N_5=8$).

The transition among decahedral structures with an axis of different length N_5 takes place always by the same mechanism. Starting, for example, from the (4,2,2) m-Dh at $N=247$ (which has $N_5=7$ atoms), an island nucleates either above the top or the bottom cap of the decahedron (see the fifth snapshot in Fig. 3, taken at $N=257$). The diffusion between top and bottom is very easy by chain processes[14,16] through the (100)-like facets, which cost 0.19, 0.13, and 0.07 eV through facets of width 3, 2, and 1, atoms respectively, so that chain processes are the most frequent interfacet processes. The jump among nearby (111)-like facets costs 0.30 eV. At high T, these barriers are frequently overcome, and an adatom can easily move around on the whole cluster [apart from being trapped in a (100)-like facet of the truncations], and single one-layer-thick island nucleates either on the top or on the bottom of the decahedron. The island is initially in *icosahedral stacking* (see, again, the fifth snapshot of Fig. 3). The icosahedral stacking breaks the perfect arrangement in columns of the decahedral structure; we have verified that this stacking is energetically favorable for islands of sizes of the order of ten atoms. When the island grows larger (see the sixth and seventh snapshots of Fig. 3), it displaces to the *decahedral stacking* (this is favorable for large islands and it restores the arrangement in columns of the structure), and the 318 (4,3,2) m-Dh (with $N_5=8$) is then completed. Icosahedral and decahedral stackings correspond respectively to hcp-like and fcc-like adsorption sites on the cluster distorted (111) facets.

On the contrary, at lower temperature, much different sequences are possible at the same (T,ϕ), and some of them lead to the growth of *metastable icosahedral structures*. Let us consider 450 K. At this temperature, the most likely growth structure around $N=150$ is already a metastable Marks decahedron, i.e., the (2,3,2) m-Dh.[7] Keeping on depositing atoms above this decahedron, icosahedral clusters can develop by two different mechanisms.

In the first mechanism (represented by the snapshots in Fig. 5; see Fig. 7 for the CNA analysis), an island on icosahedral stacking is formed, and a further island nucleates above it, due to Ehrlich, Hudda-Schwoebel[29] barriers at the outer edge of the island. Thus, an icosahedral-like facet is formed (see the second snapshot of Fig. 5); at one corner of this facet, a new fivefold axis begins to form, and then this new axis causes the transformation of the inner part of the cluster. This is what we call *two-layer-island mechanism.* Another possibility (see the snapshots in Fig. 6 and the CNA in Fig. 7) is that a large one-layer island nucleates either on the top or the bottom in icosahedral stacking, and then, contrary to what happens at 600 K, the island is not able to rearrange to the decahedral stacking because of the lower temperature. After that, the filling of a nearby Marks truncation by incoming adatoms creates a new fivefold symmetry at the cluster surface. This new fivefold symmetry propagates fast to the inner of the cluster. This is what we call *one-layer-island mechanism*. Contrary to what happens to the high-temperature Ih $\rightarrow$ Dh transformation, these intermediate-temperature Dh $\rightarrow$ Ih transformations do not involve the formation of quasimelted structures. In the one-layer-island mechanism, from a 146 (2,3,2) m-Dh, the next icosahedral structure (at $N=309$) is usually formed, while the two-layer-island mechanism leads more frequently to the growth of a larger icosahedron (which is completed at $N=561$). These mechanisms cause the growth of metastable icosahedra in most of the simulations at 450 K.

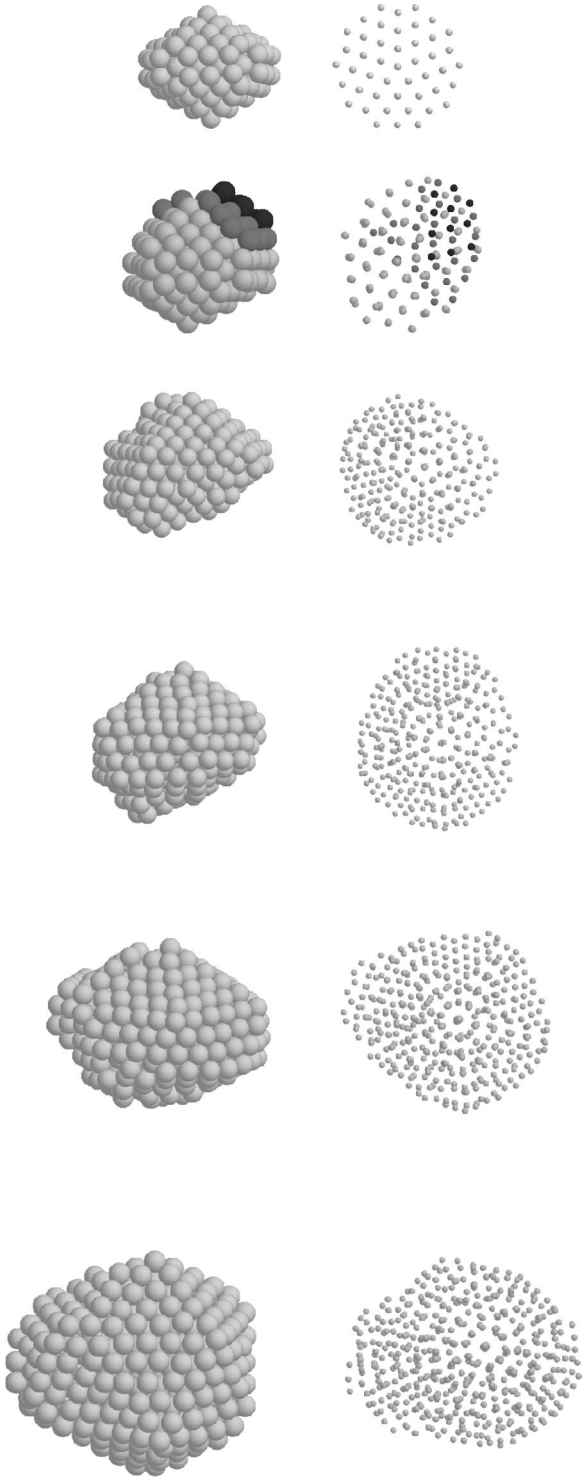

FIG. 5. Growth at 450 K, with the transformation from a metastable decahedron to a metastable icosahedron via the two-layer-island mechanism. Snapshots are taken at $N=146$, 181, 307, 388, 434, 561 atoms. A two-layer-thick island on icosahedral stacking is seen in the second snapshot (at $N=181$). After the formation of this island, a new fivefold symmetry point is formed at the cluster surface by the filling of a nearby Marks truncation. Then the fivefold symmetry propagates to the inner of the cluster, and the 561 icosahedron grows.

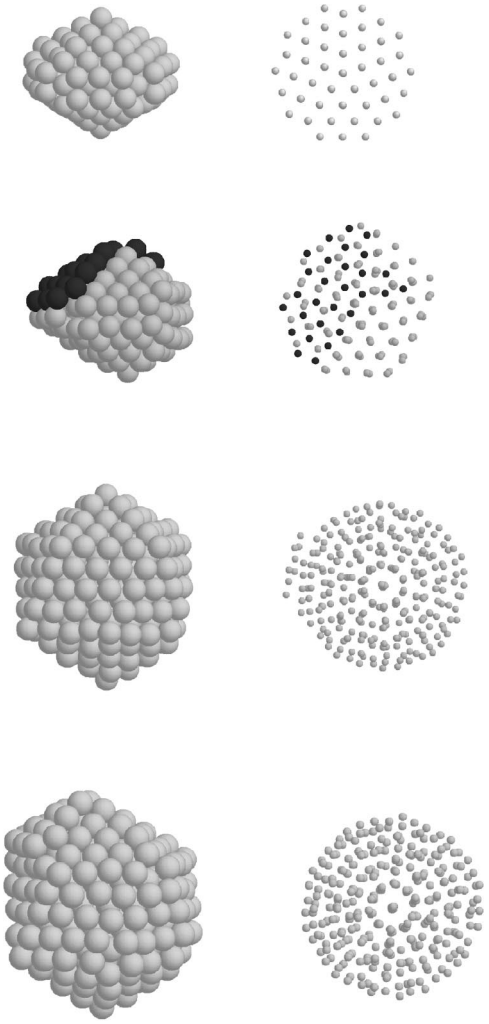

FIG. 6. Growth at 450 K, with the transformation from a metastable decahedron to a metastable icosahedron via the one-layer-island mechanism. Snapshots are taken at $N=146$, 181, 309, 324 atoms. A one-layer-thick island on icosahedral stacking is seen in the second snapshot (at $N=181$). After that, the cluster transforms into an icosahedron (the 309 icosahedron).

At 400 K, icosahedra are preferentially grown around $N=150$.[7] Keeping on depositing, some small islands nucleate on the surface of the icosahedron (the barrier from one facet to another is of 0.31 eV). These islands can either grow independently or coalesce. This can give a *shell-by-shell growth* of the icosahedron. However, we remark that even the nucleation of further islands above the first grown shell does not cause the breaking of the icosahedral symmetry, but simply, the growth of an icosahedron with more defects. On the other hand, the cluster has no chance to optimize its structure at low T; this can happen only on extremely long time scales (see the discussion in Ref. 7). In Fig. 8, we show the growth of an almost perfect 309 icosahedron, in a shell-by-shell mode. We speculate this growth mode to continue easily up to bigger sizes.[14] More importantly, the 309 and 561 icosahedral structures obtained at 450 K can continue growing by the shell-by-shell mechanism, and possibly reach the large sizes as observed in the experiments.[8]

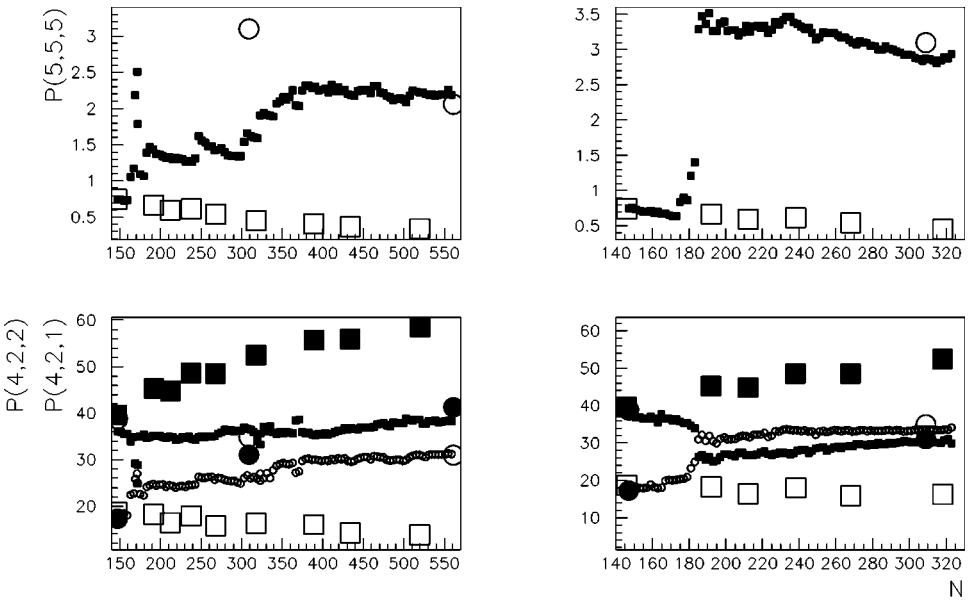

FIG. 7. Common-neighbor analysis of the simulations of Fig. 5 (left panels) and Fig. 6 (right panels). Symbols as in Fig. 4. The transition to the icosahedral symmetry takes place in both cases well below $N=200$. In the two-layer-island mechanism (left panels), two icosahedral shells are growing together, leading, thus, directly to the 561 icosahedron, while in the one-layer-island case (right panels) a single icosahedral shell is growing, and the 309 icosahedron is first formed.

V. GROWTH OF FCC CLUSTERS

Face-centered-cubic crystalline clusters have been found in our simulations, even if in a smaller proportion with respect to noncrystalline structures. We have essentially singled out two possible mechanisms for the growth of fcc clusters. The first mechanism is active at low temperatures ($T<450$ K at the fluxes of our simulations) and the second (and more important) at high temperatures ($T\simeq 650$ K). On the other hand, the growth of fcc crystallites at intermediate temperatures does not seem to be likely (we obtained it only once in several simulations).

The first mechanism, which is not frequently observed, is shown by the snapshots in Fig. 9, taken from a simulation at 400 K with a deposition interval $\tau=21$ ns. In this simulation, the 75 decahedron grows in an asymmetric way so that, around $N=110$, its fivefold axis is displaced towards the border of the structure (see the second, third, and fourth snapshots in Fig. 9). After subsequent depositions, this axis disappears (around $N=160$) with a sudden drop to zero of $P(5,5,5)$. After that, no more locally fivefold axes are created, even if the structure remains rather different from a perfect truncated octahedron [see the values of $P(4,2,2)$ and $P(4,2,1)$ in Fig. 9].

The second (high-temperature) mechanism takes place quite often; an example is shown in Fig. 10, where a simulation at 650 K with $\tau=7$ ns is reported. We recall that rather favorable symmetric truncated octahedra are found, for example, at $N=201$ and $N=314$, and in the vicinity of these magic numbers, decahedra and fcc clusters are in close competition from the energetic point of view. Moreover, there are several asymmetric truncated octahedra in between for $200<N<300$, whose energies are again in competition with those of the several (perfect or with defects) Marks decahedra that can be found in this interval. Because of that, when temperature is high enough and the energy differences become less important, the growing cluster can pass through different fcc and decahedral structures, growing finally as an fcc structure, instead of growing as a decahedron. Since the majority of the simulations at 650 K gives fcc structures for $N>280$ atoms, we may guess that the free energy of fcc clusters is lower than the free energy of decahedra at these sizes and temperatures. This indicates that the entropic contribution to the free energy becomes very important around 650 K, so that the relative stability of the structures changes with respect to the results obtained by energy optimization at 0 K. A similar effect was already pointed out in simulations of the melting of gold clusters,[30] and is currently under investigation. A study of the vibrational properties of the dif-

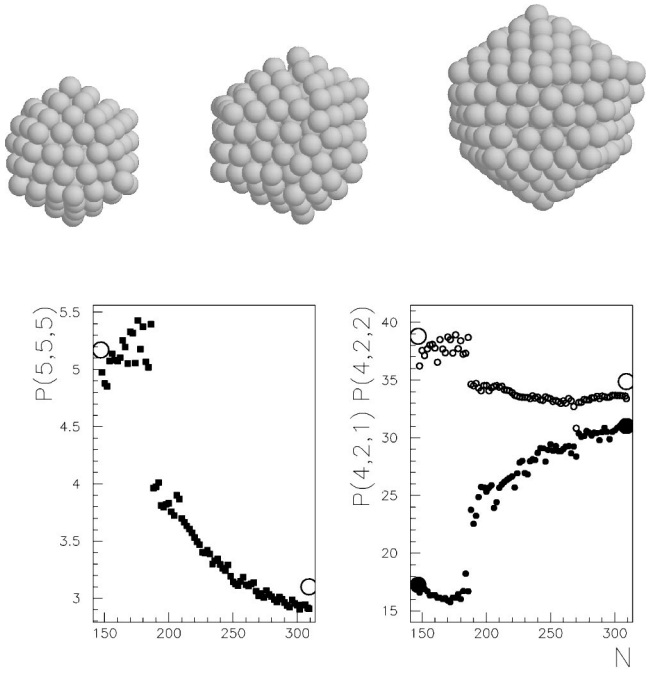

FIG. 8. Growth at 400 K. Snapshots at $N=147$, 200, 309, and CNA analysis (symbols as explained in Fig. 4). Here, the growth starts preferentially from Ih structures at $N\simeq 150$, and proceeds in a shell-by-shell mode retaining the Ih symmetry.

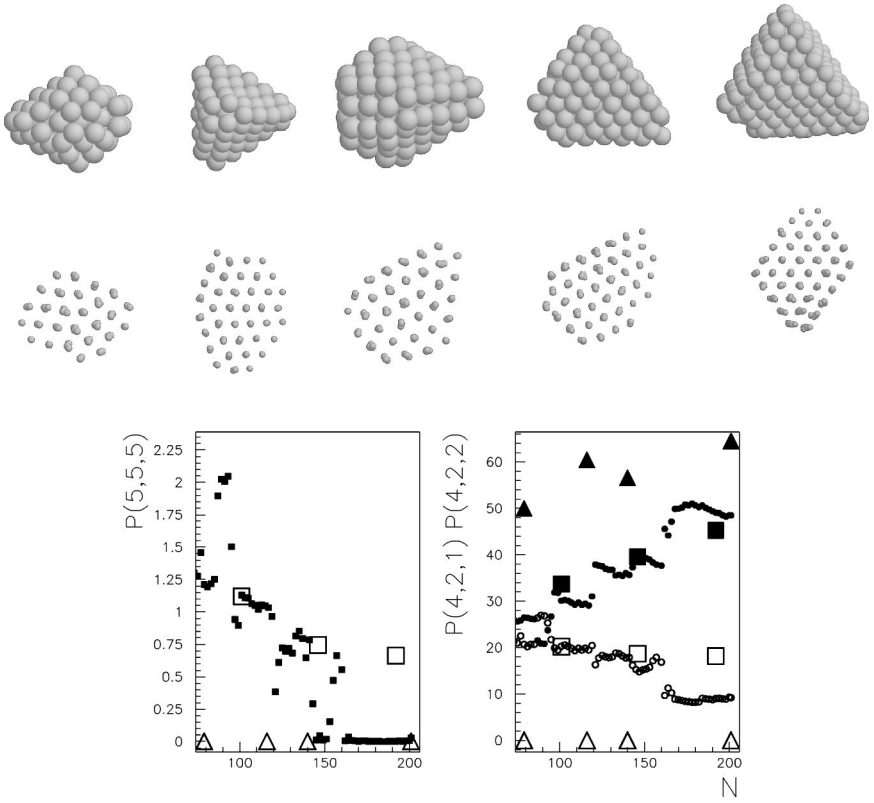

FIG. 9. Dh → fcc transformation at $T=400$ K. Snapshots at $N=75$, 114, 120, 147, 201, and CNA analysis (symbols as explained in Fig. 4). The 75 decahedron (first snapshot from left) grows asymmetrically so that the fivefold symmetry axis, which is initially more or less at the center of the structure, is displaced to the border of the cluster (see the second, third, and fourth snapshots in the top view of the second row). After that, the fivefold axis disappears (around $N=160$) with a sudden drop to zero of $P(5,5,5)$. However, the fcc structure is quite far from the symmetric truncated octahedra, as can be seen from the inspection of $P(4,2,1)$ and $P(4,2,2)$.

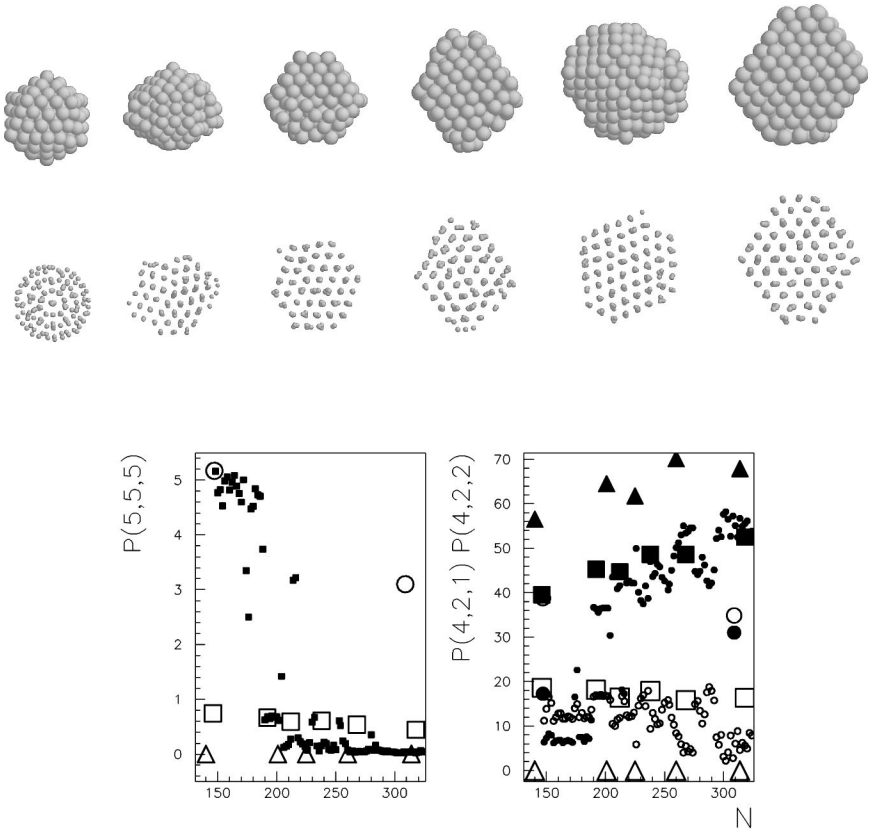

FIG. 10. Growth of fcc clusters at $T=650$ K. Snapshots at $N=147$, 188, 205, 247, 309, 318, and CNA analysis (symbols as explained in Fig. 4). From $N=147$ to $N\simeq180$, we find quasimelted structures with local fivefold symmetries. Around $N=190$ (second snapshot) the structure becomes a decahedron. Then the cluster passes through decahedra and (more frequently) fcc structures up to about 280 atoms (for example, in the third snapshot, the structure is fcc). Sometimes, defected structure with local fivefold symmetries at the border are formed (see the fourth snapshot in the top view of the second row, which looks fcc except for a locally fivefold axis, the right bottom side). After $N\simeq280$, $P(5,5,5)$ is always zero, indicating the loss of fivefold symmetries, and the structure grows as an fcc crystallite, even if, also in this case, the inspection of $P(4,2,1)$ and $P(4,2,2)$ indicates that it is quite different from a perfect truncated octahedron.

ferent clusters[31] would be of help in evaluating the entropic contribution to the free energy.

In any case, the fact that fcc clusters are more easily grown when temperature is high is in agreement with the experimental findings in Ref. 8. Finally, we could speculate that a high-temperature mechanism of the above kind could cause the transition to icosahedral clusters around $N=309$ (this is the highest size at which icosahedra have somewhat favorable energetics after quenching, according to the potential used in our simulations), but this transition has never taken place in our simulations.

VI. DISCUSSION AND CONCLUSIONS

Here we discuss the relevance of our results for the interpretation of the IGA sources experiments in Ref. 8. We recall that in these experiments, small clusters (2 nm) are mostly decahedral, intermediate-size clusters show abundances of decahedral, icosahedral and fcc structures, while (much more surprisingly) at large sizes, there is a great abundance of icosahedra, which are, in many cases, even dominant over large fcc clusters. On the other hand, large decahedra are less frequently observed. These results are clearly in contrast with energetic considerations, and suggest that the formation of these large metastable icosahedra is due to kinetic factors.[8] But now a further question arises: why are large metastable structures more frequently icosahedra than decahedra?

Our results can give a coherent answer to this question. As a first thing, we notice that, at $N>150$, we never observed low- or intermediate-T transformations from an icosahedron to a decahedron during growth, while the reverse happens rather easily (and, less frequently, also the Dh $\rightarrow$fcc transition takes place). In order to have an Ih $\rightarrow$Dh transformation, a quasimelted and short-lived intermediate structure must form, and then, a sudden complete rearrangement takes place. This can happen when T is not very far from the melting temperature of the cluster. On the contrary, it is possible to transform a decahedron into an icosahedron by creating an external incomplete icosahedral shell, and then letting the symmetry propagate to the inner. This does not require high T, and already happens for the formation of the stable 147 icosahedron from the 75 decahedron at low T.[7] However, for the Dh $\rightarrow$Ih transformation, the larger is the starting decahedron, the higher is the required T at a given flux ϕ. In fact, at $\tau=7$ ns the 75 (2,2,2) m-Dh can grow to the 147 icosahedron already at 400 K;[7] on the other hand, the transformation of the 146 (3,2,2) m-Dh into an icosahedron is mostly effective at 450 and 500 K (where, on the contrary, the 75 (2,2,2) m-Dh keeps growing as a decahedron). We expect that, at any given growth temperature, there is a size (the larger the higher is T) at which the Dh $\rightarrow$Ih transformation is likely. Because of that, if a cluster grows large, it very likely grows as an icosahedron (or, if temperature is high, as fcc), even if it starts as a decahedron at small sizes. In fact, the Dh $\rightarrow$Ih transformation is crucial since the shell-by-shell growth mode (from a very small, stable Ih) alone is not sufficient to explain why large Ih are more abundant than large Dh, as observed experimentally.

In conclusion, we summarize our results as follows. Let us consider a given flux and vary the temperature. At low and intermediate temperatures ($350<T<500$ K) the clusters grow through a sequence Ih$\rightarrow$Dh$\rightarrow$Ih, and then the icosahedron keeps growing by a shell-by-shell mode. The first Ih $\rightarrow$Dh takes place always in between $55<N<75$, while the crucial transformation Dh $\rightarrow$Ih takes place already around $N=100$ atoms if $T<400$ K and around $N=200$ atoms if $T>400$ K. In the latter case, the transformation starts from the metastable 146 m-Dh and leads to a metastable icosahedron, so that the resulting sequence is the opposite of what the energetics would suggest. On the other hand, 2 nm-size clusters are mainly decahedra in this temperature range (consider that either the 75 stable Dh or the 146 metastable Dh or the 192 stable Dh are very likely to be grown at low temperatures). At high temperatures ($T>600$ K), for $N>280$ the cluster preferentially grows as an fcc crystallite, after having passed through a decahedral regime around $N=200$. There is only a rather narrow temperature range ($500<T<600$ K) in which clusters grow as decahedra for $170<N<550$ atoms. Moreover, we cannot exclude a transformation to Ih structures at somewhat larger sizes. Unfortunately, our present computational means do not allow the simulation of significantly larger sizes. Our results are thus in good agreement with the IGA experiments in Ref. 8; in fact, we have found that it is very easy to grow small (2 nm) decahedral clusters, in a wide range of growth conditions, but the subsequent deposition of atoms can cause their transformation into icosahedra at low temperatures and fcc crystallites at high temperatures. These Dh $\rightarrow$Ih and the Dh $\rightarrow$fcc transformations lead to a reduction of the abundance of decahedra at large sizes, explaining why large icosahedra or large fcc clusters are more frequent than large decahedra in silver,[8] even if the decahedra are energetically better structures, and they are very common at small sizes. The Dh $\rightarrow$Ih transformation takes place essentially by two microscopic mechanisms, both beginning at the cluster surface, with the nucleation of islands on icosahedral stacking. The island thickness can be of one or two layers (one-layer-island or two-layer-island mechanisms), and in both cases, a new fivefold symmetry appears at the filling of a nearby Marks truncation. From the 146 (2,3,2) m-Dh, the cluster grows directly to a 561 Ih via the two-layer-island mechanism, and to a 309 Ih via the one-layer-island mechanism. Then, when a metastable icosahedron is obtained, the growth can proceed again shell by shell. The Dh $\rightarrow$fcc transformation can be obtained in a few cases at low temperatures (when asymmetric decahedra lose their fivefold axis) or, much more frequently, when temperature is high enough to overcome the rather small energy differences between decahedral and fcc structures at intermediate sizes.

ACKNOWLEDGMENTS

F. Baletto and R. Ferrando acknowledge support from the Italian MURST under Project No. 9902112831. The CRMC2 is associate to the Universities of Aix-Marseille II and III.

*Corresponding author. Email address: ferrando@fisica.unige.it

[1] C. R. Henry, Surf. Sci. Rep. **31**, 231 (1998).
[2] P. Jensen, Rev. Mod. Phys. **71**, 1695 (1999).
[3] W. Harbich, in *Metal Clusters at Surfaces*, Clusters Physics (Springer, Berlin, 2000), Chap. 4.
[4] L. D. Marks, Rep. Prog. Phys. **57**, 603 (1994).
[5] T. P. Martin, Phys. Rep. **273**, 199 (1996).
[6] W. de Heer, Rev. Mod. Phys. **65**, 611 (1993).
[7] F. Baletto, C. Mottet, and R. Ferrando, Phys. Rev. Lett. **84**, 5544 (2000).
[8] D. Reinhard, B. D. Hall, D. Ugarte, and R. Monot, Phys. Rev. B **55**, 7868 (1997).
[9] C. L. Cleveland and U. Landman, J. Chem. Phys. **94**, 7376 (1991).
[10] C. Mottet, G. Treglia, and B. Legrand, Surf. Sci. **383**, L719 (1997).
[11] C. L. Cleveland, U. Landman, T. G. Schaaff, M. N. Shafigullin, P. W. Stephans, and R. L. Whetten, Phys. Rev. Lett. **79**, 1873 (1997).
[12] K. Michaelian, N. Rendón, and I. L. Garzon, Phys. Rev. B **60**, 2000 (1999); I. L. Garzon, K. Michaelin, M. R. Beltrán, A. Posada-Amarillas, P. Ordejon, E. Artacho, D. Sánchez-Portal, and J. M. Soler, Phys. Rev. Lett. **81**, 1600 (1998); J. M. Soler *et al.*, Phys. Rev. B **61**, 5771 (2000).
[13] J. P. K. Doye and D. J. Wales, New J. Chem. **22**, 733 (1998); Chem. Phys. Lett. **247**, 339 (1995); S. Erkoc and T. Yilmaz, Physica E **5**, 1 (1999).
[14] S. Valkealahti and M. Manninen, Phys. Rev. B **57**, 15 533 (1998); Z. Phys. D: At., Mol. Clusters **40**, 496 (1997).
[15] M. Guillopé and B. Legrand, Surf. Sci. **215**, 577 (1989).
[16] F. Baletto, C. Mottet, and R. Ferrando, Surf. Sci. **446**, 31 (2000).
[17] F. Montalenti and R. Ferrando, Phys. Rev. B **59**, 5881 (1999).
[18] G. A. Evangelakis and N. I. Papanicolaou, Surf. Sci. **347**, 376 (1996); D. G. Papageorgiou and G. A. Evangelakis, *ibid.* **461**, L543 (2000).
[19] R. Ferrando and G. Tréglia, Phys. Rev. B **50**, 12 104 (1994); Phys. Rev. Lett. **76**, 2109 (1996); R. Ferrando, *ibid.* **76**, 4195 (1996); F. Montalenti and R. Ferrando, *ibid.* **82**, 1498 (1999).
[20] O. S. Trushin, M. Kotrla, and F. Maca, Surf. Sci. **389**, 55 (1997).
[21] G. Prevot, C. Cohen, D. Schmaus, and V. Pontikis, Surf. Sci. **459**, 57 (2000).
[22] F. Picaud, C. Ramseyer, C. Girardet, and P. Jensen, Phys. Rev. B **61**, 16 154 (2000).
[23] V. S. Stepanyuk, D. I. Bazhanov, and W. Hergert, Phys. Rev. B **62**, 4257 (2000).
[24] D. Reinhard, B. D. Hall, P. Berthoud, S. Valkealahti, and R. Monot, Phys. Rev. Lett. **79**, 1459 (1997).
[25] H. Jonsson, G. Mills, and K. W. Jacobsen, in *Classical and Quantum Dynamics in Condensed Phase Simulations*, edited by B. J. Berne, G. Ciccotti, and D. F. Coker (World Scientific, Singapore, 1998).
[26] D. Faken and H. Jónsson, Comput. Mater. Sci. **2**, 279 (1994).
[27] C. L. Cleveland, W. D. Luedtke, and U. Landman, Phys. Rev. B **60**, 5065 (1999).
[28] F. Baletto, F. Montalenti, C. Mottet, and R. Ferrando (unpublished).
[29] G. Ehrlich and F. G. Hudda, J. Chem. Phys. **44**, 1039 (1966); R. L. Schwoebel, J. Appl. Phys. **40**, 614 (1968).
[30] C. L. Cleveland, W. D. Luedtke, and U. Landman, Phys. Rev. Lett. **81**, 2036 (1998).
[31] A. Kara and T. S. Rahman, Phys. Rev. Lett. **81**, 1453 (1998).